Published in Materials Science and Engineering B 59, issues 1-3, 33-38, 1999
which should be used for any reference to this work



# MOCVD growth and characterization of AlGaInN multiple quantum well heterostructures and laser diodes

D.P. Bour *, M. Kneissl, D. Hofstetter, L.T. Romano, M. McCluskey, C.G. Van de Walle, B.S. Krusor, C. Dunnrowicz, R. Donaldson, J. Walker, N.M. Johnson

*Electronic Materials Laboratory, XEROX Palo Alto Research Center, Palo Alto, CA 94304, USA*

**Abstract**

We demonstrate room temperature, pulsed, current-injected operation of InGaAlN heterostructure laser diodes with mirrors fabricated by chemically assisted ion beam etching. The multiple quantum well devices were grown by organo–metallic vapor phase epitaxy on c-face sapphire substrates. The emission wavelengths of the gain-guided laser diodes were $\sim 400$ nm. The lowest threshold current density obtained was 6 kA $cm^{-2}$ with maximum output powers of 50 mW per facet. Optically-pumped distributed-feedback laser operation was also achieved.

*Keywords:* Semiconductor lasers; CVD; Nitrides; Epitaxial deposition; Quantum well semiconductor epitaxial layers; Quantum well lasers; Semiconductor heterojunctions

## 1. Introduction

The rapid development of efficient, visible light emitting diodes (LEDs) from nitride semiconductors has had a tremendous impact on many important systems technologies [1,2]. For example, blue and green nitride LEDs are now the basis of bright, full-color displays, when combined with existing red LEDs. In this application, the efficiency and color purity of the LEDs permit a very broad range of colors to be mixed, spanning a substantial portion of all perceived colors. Moreover, since white light can be generated through such color mixing, or by using UV-blue LEDs to excite various color phosphors, LEDs are now also being considered for general illumination.

The spectacular success of nitride LEDs, particularly their efficiency, color purity, and reliability, has also provided an incentive to pursue nitride laser diodes. Similar to the application of LEDs in full-color displays, a combination of primary-color lasers may also be incorporated in full-color film printers and projection displays. Still another primary motivation for developing cheap, compact nitride semiconductor laser diodes is optical data storage, where a short wavelength translates into a small focused spot size, as required for maximizing the density and transfer rate of stored data. High-resolution printing enjoys a similar advantage from short-wavelength lasers.

Over the past 2–3 years, blue semiconductor lasers have undergone tremendously rapid development at Nichia [3–15]. Lifetimes exceeding 10 000 h have been projected for low-power (2 mW), single-mode, self-pulsing lasers. These performance characteristics are suitable for incorporation in DVD-ROM systems; but higher powers are still required for DVD-recordable systems and for high-speed, high-resolution laser printers. Accordingly, this paper is a description of our epitaxial growth, characterization, and processing of nitride materials and heterostructures, from which we have obtained room temperature, pulsed operation of nitride laser diodes.

## 2. OMVPE growth and nitride material characterization

Nitride semiconductor films were grown by organo–metallic vapor phase epitaxy (OMVPE). Precursors in-

* Corresponding author.

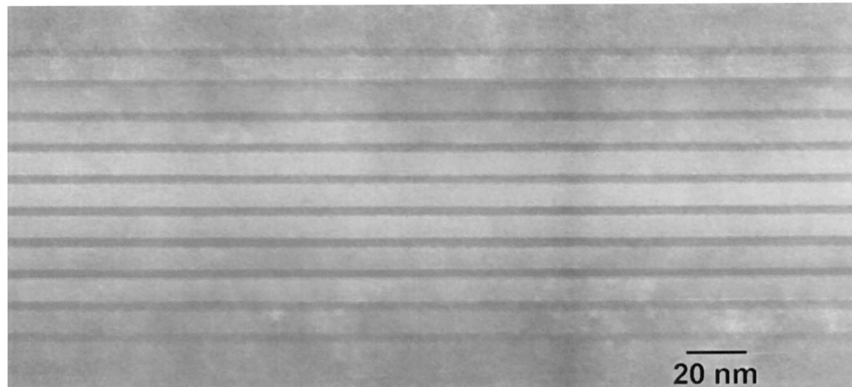


Fig. 1. Transmission electron microscope image showing the multiple quantum well active region of an InGaN/GaN laser diode structure.

cluded trimethyl -gallium, -indium, and -aluminum, triethylgallium (used for quantum well growth), biscyclopentadienylmagnesium, dilute (10 ppm) silane, and purified ammonia. Growth was performed over c-face (0001) sapphire substrates, beginning with a thin (30 nm) low-temperature (550°C) GaN nucleation layer, as is typically described in the literature [1,3,6,8]. The device structures are similar to those described by Nakamura et al., and include a 4 μm GaN:Si lateral n-contact layer, a 0.4 μm $Al_{0.08}Ga_{0.92}N$:Si cladding layer, and a 3, 5, or 10 InGaN multiple quantum well (MQW) active region surrounded by 0.1 μm GaN:Si and GaN:Mg waveguide layers. This is followed by a 0.4 μm $Al_{0.08}Ga_{0.92}N$:Mg cladding layer, topped with a 0.1 μm GaN:Mg p-contact layer [3–6,9–16].

Adequate levels of p-type doping are essential for the successful operation nitride lasers. We have performed a comprehensive theoretical investigation of acceptor doping in GaN, using first-principles calculations based on density-functional theory and ab initio pseudopotentials [17]. Incorporation of Mg on interstitial or substitutional nitrogen sites has often been invoked to explain limited hole concentrations; however, the calculations show that this type of incorporation is energetically unfavorable [18]. We found that the determining factor is the solubility of Mg in GaN, which is limited by competition between incorporation of Mg acceptors and formation of $Mg_3N_2$.

We have also performed an extensive computational investigation of other acceptor impurities in GaN [19]. None of the candidate impurities (Na, Li, Be, Ca, Zn, and C) exhibit characteristics superior to Mg. Only Be has a comparable solubility and a potentially lower ionization energy. Be doping is likely to be severely hampered, however, by the incorporation of Be donors on interstitial sites. A certain degree of compensation by native defects does occur in p-type GaN, in particular by nitrogen vacancies; and this compensation becomes increasingly severe for increasing Al content in AlGaN alloys [20,21]. In addition, we calculate an increase in the ionization energy of the Mg acceptor with increasing Al content. These factors explain the increased difficulty in p-type doping of AlGaN.

In addition to p-type doping, the structural and optoelectronic quality of the InGaN MQW active region is critically important in achieving nitride laser operation. The structural quality of the ten $In_{0.2}Ga_{0.8}N$/GaN multiple quantum wells of a laser diode structure is apparent in the transmission electron microscope (TEM) image shown in Fig. 1. The layer thicknesses are uniform, with sharp interfaces between the InGaN QWs and GaN barriers. From this micrograph, the layer thicknesses are determined to be 2.5 nm for the InGaN well layers, and 6 nm for the GaN barriers.

Fig. 2 shows the X-ray diffraction spectrum of an MQW active region, like that which has been incorporated into InGaN laser diodes (but with no AlGaN cladding layers). This structure contains ten 2 nm $In_{0.2}Ga_{0.8}N$ QWs, separated by 5 nm GaN barriers. Evidence of the layer uniformity is indicated by coher-

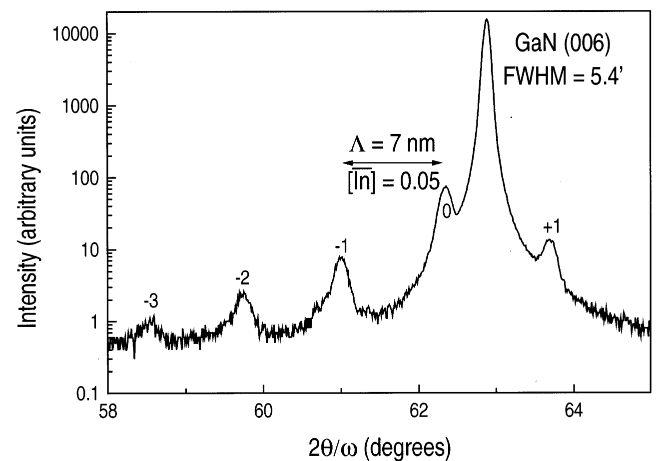


Fig. 2. (006) X-ray diffraction pattern of a InGaN/GaN 10-QW structure.

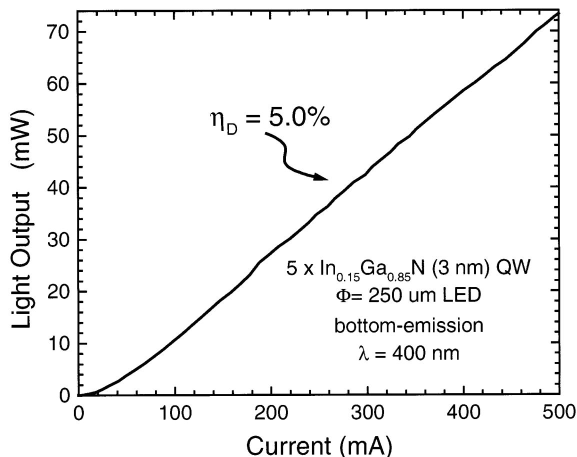


Fig. 3. *L–I* characteristic of a 400 nm, InGaN/GaN 5-QW laser diode structure tested as an LED.

ent reflections from the periodic multilayers comprising the active region, which give rise to visible (±)1st, (−)2nd, and (−)3rd -order satellite peaks in the XRD spectrum. The presence of these peaks in the XRD spectrum demands that the superlattice structure be highly periodic. The spacing of the satellite peaks indicates the period of the superlattice active region to be ~70 Å. Likewise, the absolute position of the 0th-order peak indicates the average InGaN composition to be ~$In_{0.05}Ga_{0.95}N$.

## 3. LED characteristics

The spectral purity and brightness of a laser diode wafer's electroluminescence, measured at current densities well below threshold, is a useful diagnostic tool for rapidly assessing the quality of materials and heterostructures, with a device structure that is much simpler to fabricate than a laser diode. Accordingly, simple 250 μm dot LEDs were fabricated from laser diode heterostructures by depositing Ti/Au p-contact metal, and dry-etching down to the 4 μm n-type GaN layer underlying the heterostructure, thereby defining 250 μm dots.

The pulsed power output (spontaneous emission) of a 5 × 3 nm $In_{0.15}Ga_{0.85}N$/GaN QW laser diode heterostructure, measured for this geometry where only the light emitted through the bottom of the wafer is detected, is shown in Fig. 3 as a function of the injection current. The electroluminescence spectrum was peaked

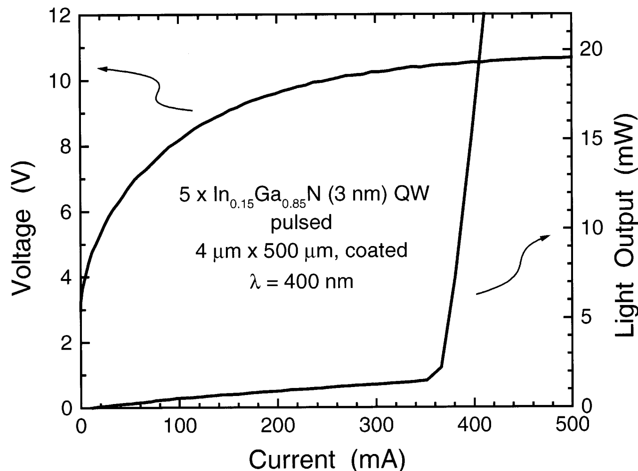


Fig. 5. Measured current–voltage and current–light output power for a 4 × 500 $\mu m^2$ laser diode (coated mirrors).

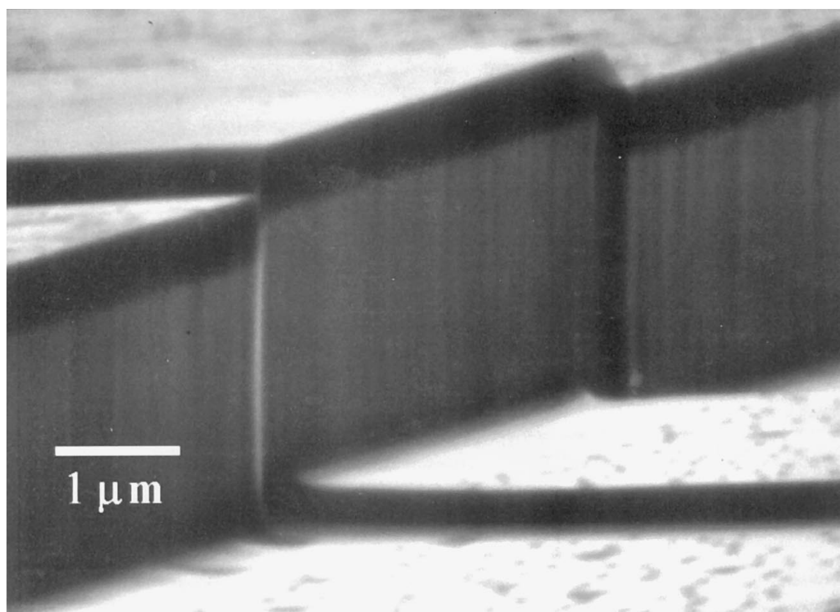


Fig. 4. Scanning-electron micrograph of nitride laser mirror fabricated by CAIBE.

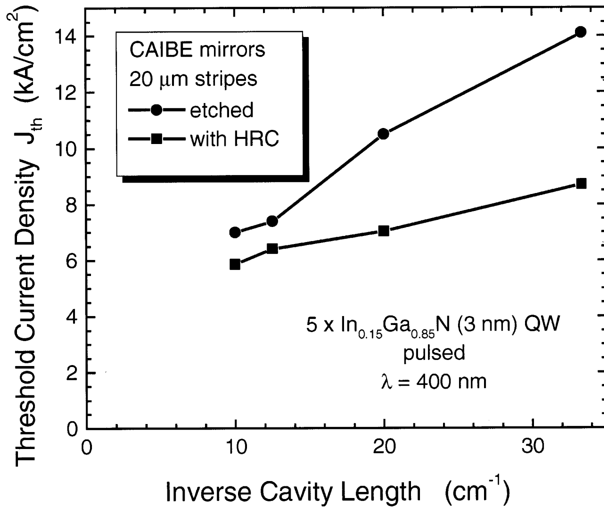


Fig. 6. Measured threshold current density for gain-guided InGaN/AlGaN laser diodes vs. the inverse cavity length. The p-metal stripe width of the broad area test structures was 20 μm; comparison for uncoated (as-etched) and coated (HRC) mirrors.

at 400 nm, and the bottom-emitted power exceeds 70 mW at 500 mA, with a differential quantum efficiency of 5%. The emission spectrum of this LED was also very pure, with a single peak over four decades of injection current, and with a full width at half-maximum of 11 nm. In contrast, some structural deterioration, possibly, but not necessarily alloy segregation, is evident when the QWs are made either thicker, with higher indium content, or more numerous. In these cases, structural defects are reflected in spectrally broad emission, which may also undergo large (sometimes discontinuous) shifts to shorter wavelengths as the injection current is increased

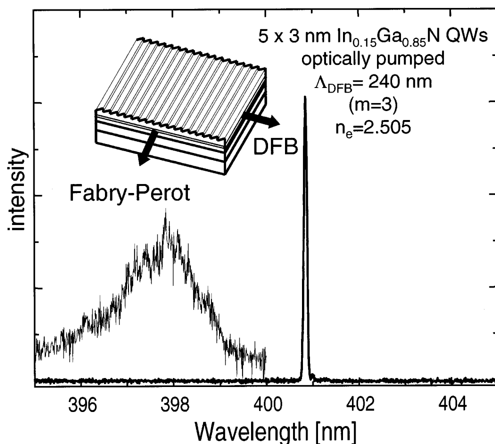


Fig. 7. F–P and DFB spectra for optically pumped laser with a holographically-defined 3rd-order grating etched into the upper waveguide.

## 4. Laser diode characteristics

We have observed pulsed-injection laser oscillation at room temperature, with an InGaN/AlGaN multiple QW heterostructure similar to those described by Nakamura et al. [3–6]. Gain-guided devices were fabricated using silicon oxy-nitride dielectric insulating layers, with stripe openings of 4, 10, or 20 μm. Both n- and p-contact metallizations were made using Ti/Au. Mirrors were etched using chemically-assisted ion beam etching (CAIBE) to define cavity lengths of 300, 500, 800, or 1000 μm. In the CAIBE technique, the mechanical etching component (Ar-ion milling current and acceleration voltage) and the chemical etching component ($Cl_2/BCl_3$ reactive gas flows and wafer temperature) are independently adjustable [23]. By optimizing these parameters, combined with the proper wafer tilt angle, vertical and smooth laser mirrors can be realized [14,23,24], as shown in Fig. 4. Moreover, the etch rate can be relatively composition-independent, thus minimizing the possibility of steps being produced at the heterostructure interfaces. Surface profiles of CAIBE-etched mirrors, measured using atomic force microscopy, reveal an RMS roughness of 4–5 nm. Based on optical pumping experiments, the reflectivity of these mirrors is estimated to be $\sim 70\%$ of the ideal value [14]. Presumably, some fraction of the incident light is scattered by the slight surface roughness, which is currently limited by the photo-resist mask. In principle, more sophisticated, multi-layer etch masks could be used to produce even smoother mirrors using CAIBE.

The light-output intensity ($L$) is shown as a function of the injection current ($I$) in Fig. 5, for a $4 \times 500$ μm diode operated pulsed at room temperature (pulse width = 500 ns, repetition rate = 10 kHz), with coated mirrors. This laser contained five, 3 nm $In_{0.15}Ga_{0.85}N$ QWs, for emission at 400 nm. The $L$–$I$ characteristic exhibits a threshold current of $\sim 0.38$ A, corresponding to a threshold current density of $\sim 19$ kA cm$^{-2}$. Above threshold, the differential quantum efficiency is 14% per facet (this value probably represents a conservative estimate of the efficiency, since it is difficult to collect all the emission from such an etched-facet device). The emission was TE-polarized and at threshold, the far-field emission pattern collapsed into a beam characteristic of an etched-facet laser. Specifically, the transverse far-field pattern exhibited a strong modulation, arising from interference between the directly-emitted beam and the component of the beam which was reflected from the etched surface, similar to that of the first nitride laser diode demonstrated by Nakamura et al., which also had etched facets [3]. The voltage ($V$)–current ($I$) characteristic is also shown in Fig. 5. The threshold voltage is $\sim 10$ V.

The threshold current density was found to have a fairly strong dependence on the cavity length ($L$), espe-

cially for lasers with uncoated mirrors. This is shown in Fig. 6, the threshold current density as a function of the inverse cavity length (since the mirror loss component of the total loss is proportional to $1/L$), for lasers with 20 μm stripe width. Comparing the cases of high-reflection-coated (HRC) and uncoated (as-etched) mirrors, the threshold is lower for devices with the reflective facet coatings applied to the mirror. The minimum threshold current density is approximately 6 kA $cm^{-2}$ for $1/L = 10$ $cm^{-1}$ ($L = 1000$ μm), and a reflective mirror-coating. The threshold's variation with cavity length ($L$) suggests that the distributed loss ($\alpha$, which comprises scattering by dislocations or waveguide irregularities, absorption loss to free carriers or the p-contact metal, outcoupling loss, etc.) is not so high as to overwhelm the mirror loss ($= 1/L \ln\{1/R\}$, where $R$ is the mirror reflectivity.

Among the many laser wafers tested, we have observed lasers from structures with either 3, 5, or 10 QWs at wavelengths between 389 and 433 nm. The lowest thresholds occurred near 400 nm.

## 5. Optically pumped, distributed feedback laser

Although most applications of nitride lasers do not require single-longitudinal-mode operation, distributed Bragg reflectors (DBRs) remain a viable alternative to etched or cleaved mirrors. In addition to their wavelength stability, another advantage includes the ability to realize a high effective reflectivity, and the potential for surface emission. We have therefore fabricated distributed-feedback (DFB) gratings in nitride laser structures, and observed oscillation based on the grating reflection during optical pumping, as shown in Fig. 7.

The DFB laser structure was fabricated from a 5 × 3 nm $In_{0.15}Ga_{0.85}N$ MQW laser wafer that was grown without a p-AlGaN upper cladding layer. Furthermore, the upper waveguide layer was made slightly thicker than normal, to accommodate the grating. Using holographic lithography with a 325 nm HeCd laser, a diffraction grating with period $\Lambda = 240$ nm was etched (by CAIBE) into the upper waveguide layer. This grating period produces reflection in the 3rd order, near the 400 nm peak of the gain spectrum. Optical pumping was performed using a pulsed 337 nm $N_2$ laser whose light was focused on a 100 μm wide by 4 mm long stripe.

By aligning the pump stripe orthogonal to the grating grooves, DFB laser action was observed, while Fabry–Perot (F–P) oscillation was recorded when the pump stripe was aligned along the grating grooves [22]. These DFB and F–P laser spectra may be compared in Fig. 7. The F–P spectrum is peaked at 398 nm and is relatively broad ($\sim 2$ nm). However, this represents a typical width for the F–P oscillation, since emission occurs in many longitudinal modes. Individual spectral modes cannot be resolved in the F–P spectrum, because of the long cavity length, operation under fast pulse conditions, and the superposition of families of longitudinal modes which are probably present for this broad-area pumping scheme. In contrast, the DFB emission is at a slightly longer wavelength of 401 nm; and it exhibits superior spectral purity compared to the F–P emission.

## 6. Summary

In summary, we have achieved room temperature, pulsed operation of InGaAlN heterostructure laser diodes with mirrors fabricated by chemically assisted ion beam etching. The devices were grown by organo–metallic vapor phase epitaxy (OMVPE) on c-face sapphire substrates. The best device structures contain five 30 Å $In_{0.15}Ga_{0.85}N$ QWs and $Al_{0.08}Ga_{0.92}N$ cladding layers. The structural and optoelectronic quality of the InGaN MQW active region is evident in TEM, spectrally pure spontaneous emission, and satellite peaks appearing in the X-ray diffraction spectrum. The emission wavelengths of the gain-guided laser diodes were in the range from 389 to 433 nm. The lowest threshold current density obtained was 6 kA $cm^{-2}$ with maximum pulsed output powers of 50 mW per facet, at a wavelength of 400 nm. Optically-pumped distributed-feedback laser operation was also achieved.

## Acknowledgements

The authors are pleased to acknowledge helpful discussions with R.D. Bringans and we thank F. Endicott and E. Taggart for technical support. This work was partially supported by DARPA under contract number MDA972-96-0014 (Blue BAND II) and DOC under contract number 70NANB2H1241.

## References

[1] S. Nakamura, M. Senoh, N. Iwasa, S. Nagahama, Appl. Phys. Lett. 67 (1995) 1868–1870.
[2] S. Nakamura, IEEE Circuits Devices (1995) 19–23.
[3] S. Nakamura, M. Senoh, S. Nagahama, N. Iwasa, T. Yamada, T. Matsushita, H. Kiyoku, Y. Sugimoto, Jpn. J. Appl. Phys. 35 (1996) 74–76.
[4] S. Nakamura, M. Senoh, S. Nagahama, N. Iwasa, T. Yamada, T. Matsushita, Y. Sugimoto, H. Kiyoku, Appl. Phys. Lett. 69 (1996) 4056–4058.
[5] S. Nakamura, M. Senoh, S. Nagahama, N. Iwasa, T. Yamada, T. Matsushita, Y. Sugimoto, H. Kiyoku, Appl. Phys. Lett. 69 (1996) 1477–1479.
[6] S. Nakamura, IEEE J. Sel. Topics Quantum Electron. 3 (1996) 712–718.

[7] I. Akasaki, H. Amano, S. Sota, H. Sakai, T. Tanaka, M. Koike, Jpn. J. Appl. Phys. 34 (1995) 1517–1519.
[8] I. Akasaki, H. Amano, J. Electrochem. Soc. 141 (1994) 2266–2271.
[9] K. Itaya, M. Onomura, J. Nishio, L. Sugiura, S. Saito, M. Suzuki, J. Rennie, S. Nunoue, M. Yamamoto, H. Fujimoto, Y. Kokobun, Y. Ohba, G. Hatakoshi, M. Ishikawa, Jpn. J. Appl. Phys. 35 (1996) 1315–1317.
[10] A. Kuramata, K. Domen, R. Soejima, K. Horino, S. Kubota, T. Tanahashi, J. Cryst. Growth 189/190 (1998) 826–830.
[11] J. Edmond, G. Bulman, H. S. Kong, M. Leonard, K. Doverspike, W. Weeks, J. Niccum, S. Sheppard, G. Negley, D. Slater, Proc. Int. Conf. Nitride Semiconductors (ICNS–97) (1997) 448–449.
[12] M.P. Mack, A.C. Abare, M. Aizcorbe, P. Kozodoy, S. Keller, U. Mishra, L.A. Coldren, S.P. DenBaars, J. Cryst. Growth 189/190 (1998) 837–840.
[13] F. Nakamura, T. Kobayashi, T. Asatsuma, K. Funato, K. Yanashima, S. Hashimoto, K. Naganuma, S. Tomioka, T. Miyajima, E. Morita, H. Kawai, M. Ikeda, J. Cryst. Growth 189/190 (1998) 841–845.
[14] M. Kneissl, D. Hofstetter, D.P. Bour, R. Donaldson, J. Walker, N.M. Johnson, J. Cryst. Growth 189/190 (1998) 846–849.
[15] S. Nakamura, M. Senoh, S. Nagahama, N. Iwasa, T. Yamada, T. Matsushita, H. Kiyoku, Y. Sugimoto, T. Kozaki, H. Umemoto, M. Sano, K. Chocho, J. Cryst. Growth 189/190 (1998) 820–825.
[16] W. Götz, N.M. Johnson, J. Walker, D.P. Bour, R.A. Street, Appl. Phys. Lett. 68 (1996) 667–669.
[17] J. Neugebauer, C.G. Van deWalle, Phys. Rev. B 50 (1994) 8067.
[18] J. Neugebauer, C.G. Van deWalle, Proc. Mater. Res. Soc. Symp. 395 (1996) 645.
[19] J. Neugebauer, C.G. Van de Walle, Proc. ICPS-23, World Scientific, Singapore, 1996, pp. 2849.
[20] J. Neugebauer, C.G. Van deWalle, Appl. Phys. Lett. 68 (1996) 1829–1831.
[21] C. Stampfl, C.G. Van deWalle, Appl. Phys. Lett. 72 (1998) 4.
[22] I. Adesida, A.T. Ping, C. Youtsey, T. Dow, M.A. Khan, D.T. Olsen, J.N. Kuznia, Appl. Phys. Lett. 65 (1994) 889–891.
[23] M. Kneissl, D.P. Bour, N.M. Johnson, L. Romano, B. Krusor, R. Donaldson, J. Walker, C. Dunnrowicz, R. Bringans, Appl. Phys. Lett. 72 (1998) 1539–1541.
[24] D. Hofstetter, R.L. Thornton, M. Kneissl, D.P. Bour, C. Dunnrowicz, Appl. Phys. Lett. 73 (1998) 1928–1930.